1989

Transition State Structure, Barrier Height, and Vibrational Frequencies for the Reaction Cl+CH4→CH3+HCl

Thanh N. Truong, *University of Minnesota - Twin Cities*
Donald G. Truhlar, *University of Minnesota - Twin Cities*
Kim K. Baldridge
Mark S. Gordon
Rozeanne Steckler

AIP | The Journal of Chemical Physics

Transition state structure, barrier height, and vibrational frequencies for the reaction Cl+CH4→CH3+HCl

Thanh N. Truong, Donald G. Truhlar, Kim K. Baldridge, Mark S. Gordon, and Rozeanne Steckler

Citation: The Journal of Chemical Physics **90**, 7137 (1989); doi: 10.1063/1.456244
View online: http://dx.doi.org/10.1063/1.456244
View Table of Contents: http://scitation.aip.org/content/aip/journal/jcp/90/12?ver=pdfcov
Published by the AIP Publishing

Transition state structure, barrier height, and vibrational frequencies for the reaction $Cl + CH_4 \rightarrow CH_3 + HCl$

Thanh N. Truong and Donald G. Truhlar
Department of Chemistry and Supercomputer Institute, University of Minnesota, Minneapolis, Minnesota 55455
Kim K. Baldridge and Mark S. Gordon
Department of Chemistry, North Dakota State University, Fargo, North Dakota 58105
Rozeanne Steckler
San Diego Supercomputer Center, San Diego, California 92138-5608

(Received 28 December 1988; accepted 16 February 1989)

We have carried out *ab initio* calculations using second- and fourth-order Møller–Plesset perturbation theory, scaled electron correlation, and several basis sets for the reaction $Cl + CH_4 \rightarrow CH_3 + HCl$. We found that including electron correlation is essential for obtaining accurate barrier heights and vibrational frequencies. Furthermore, scaling the correlation energy further improves the barrier height predictions provided that the basis set being used is correlation balanced for both bonds involved in the reaction. Geometries and transition state frequencies calculated at the MP2 and MP-SAC2 levels with the most extensive and best balanced basis set are in good agreement with one another for all bound modes, but the unbound-mode frequency changes by $214i$ cm^{-1}.

I. INTRODUCTION

The reaction of $Cl(^2P)$ with methane,

$$Cl(^2P) + CH_4 \rightarrow HCl \rightarrow CH_3, \quad (R1)$$

removes Cl atoms from the Cl/ClO chain which catalytically destroys ozone in the earth's stratosphere.[1] By forming the relatively stable HCl molecule, reaction (R1) serves as a major sink for Cl atoms in the stratosphere. For this reason, many experimental investigations of this reaction have been carried out in recent years[2–6] (references given here are only representative, not exhaustive), and the rate constant has been measured over a broad range of temperature. However, theoretical dynamical studies of this reaction are very limited and highly approximate,[5,7] due to the lack of an accurate potential-energy surface (PES) for this sytem. Construction of the PES requires information about the saddle-point geometry and vibrational frequencies, for a start, and about the whole reaction swath,[8] for further progress. Such information is in principle available from *ab initio* calculations, but, to the best of our knowledge, there are no published *ab initio* studies of the reaction $Cl + CH_4$. Thus, because of the intrinsic interest in this reaction for atmospheric studies and also because it can serve as a prototype for other atmospheric and combustion reactions, we have undertaken such a study. In addition to the intrinsic interest in these reactions, the calculations may be of general interest because they shed new light on the basis set sizes required to calculate accurate barrier heights for chemical reactions.

In the present study, we have calculated the structures and energetics of the reactants, products, and saddle point for reaction (R1). The barrier heights for both the forward and backward directions of reaction, and the vibrational analysis at the stationary structures are discussed. We employ second- and fourth-order Møller–Plesset [MP2 (Ref. 9) and MP4 (Ref. 10)] perturbation theory, based on restricted and unrestricted Hartree–Fock (HF) reference states. In addition we extrapolate to complete basis sets and full inclusion of correlation energy by "scaling all correlation" [SAC (Ref. 11)] energy in the MP2 and MP4 calculations, yielding semitheoretical estimates of the true barrier heights labeled MP–SAC2 and MP–SAC4, respectively.

II. COMPUTATIONAL METHODOLOGY

All HF calculations for systems with an even number of electrons are restricted to doubly occupied orbitals and those for odd numbers of electrons are unrestricted, i.e., they involve different orbitals for different spins. The geometries of all minimum energy structures and transition states were fully optimized using analytical gradients, using different point group symmetries for different species, i.e., $C_{\infty v}$ for HCl, D_{3h} for CH_3, T_d for CH_4, and C_{3v} for the Cl–H–CH_3 saddle point.

We used several basis sets in the present study, in particular, the 3–21G** basis,[12] in which *d* functions are added to Cl but not C, and a set of *p* functions are added to H; the 6–31G** basis,[12] where *d* functions are included on both C and Cl and *p* functions are included on H; the 6–31 + G** basis,[13] where, in addition, a set of diffuse *s* and *p* functions is added to each heavy atom, C and Cl; and two more extended basis sets, denoted MC–311G(*d,d,p*) and MC–311G(2*d,d,p*). In the latter basis sets, we have combined the 6–311G** basis[14] for carbon, the 311G** basis[14] for hydrogen, and McLean–Chandler basis[15] for chlorine. These extended basis sets for the valence symmetries were augmented with one set of polarizations functions on each atom for MC–311G(*d,d,p*), and also with a second set of *d* functions on Cl for MC–311G(2*d,d,p*). The *d* function exponential parameter used in the MC–311G(*d,d,p*) basis is 0.75.[12] For

0021-9606/89/127137-06$02.10

the MC–311G(2*d*,*d*,*p*) basis, we have optimized the two Cl *d*-function exponential parameters with respect to the HCl total energy at the correlated MP2 level, and we have values of 1.04 and 0.34, respectively. (The reason for optimizing these exponents at MP2 instead of the HF level will be discussed in a later section.) Six Cartesian *d* functions were used in all *d* sets.

We have performed both HF and MP2 calculations in predicting the structures and transition state vibrational frequencies. Single-point energy calculations were also carried out using full fourth-order Møller–Plesset perturbation theory, MP4 (SDTQ),[10] at the MP2 structures using the 6–31G** and MC–311G(*d*,*d*,*p*) basis sets. The inner-shell as well as the valence-shell electrons are correlated in all MP2 and MP4 calculations.

Finally, to improve the energy predictions for the saddle points, we have scaled all the correlation (SAC) energy of the Møller–Plesset perturbation theory results. Scaling the MP2 and MP4 results yields extrapolated energies called[11] MP–SAC2 and MP–SAC4, respectively.

The HF and MP calculations and the MP–SAC single-point calculations were carried out using the GAUSSIAN82 (Ref. 16) program on a Cray-2 computer at the Minnesota Supercomputer Institute, the Cray X-MP/48 computer at the Pittsburgh Supercomputing Center, and a VAX 8530 computer at North Dakota State University. The MP–SAC geometry optimizations were calculated using a locally modified version of GAUSSIAN82 on the VAX 8530, and the MP–SAC frequencies were calculated using a locally modified GAUSSIAN86 (Ref. 17) on the Cray X-MP/48 computer at the San Diego Supercomputer Center.

III. RESULTS AND DISCUSSION

A. Structures and vibrational frequencies

The calculated equilibrium and transition state geometries are given in Tables I and II. First we note that the HF bond lengths of the equilibrium structures are generally shorter than their experimental values; however, the bond lengths of HCl and CH_4 predicted at the MP2/MC–311G(2*d*,*d*,*p*) and MP–SAC2/MC–311G(2*d*,*d*,*p*) level are in excellent agreement with the available experimental[18,19] values.

TABLE I. Optimized minimum energy structures (bond length in Å).

Species Bond	HCl($C_{\infty v}$) H–Cl	CH_3(D_{3h}) C–H	CH_4(T_d) C–H
HF/3–21G**	1.2672	1.0710	1.081 6
HF/6–31G**	1.2654	1.0728	1.083 5
HF/6–31 + G**	1.2662	1.0729	1.088 39
HF/MC–311(*d*,*d*,*p*)	1.2680	1.0735	1.084 2
HF/MC–311(2*d*,*d*,*p*)	1.2681	1.0842	1.084 2
MP2/6–31G**	1.2684	1.0735	1.084 3
MP2/6–31 + G**	1.2687	1.0744	1.085 1
MP2/MC–311G(*d*,*d*,*p*)	1.2740	1.0786	1.089 4
MP2/MC–311G(2*d*,*d*,*p*)	1.2747	1.0786	1.089 4
MP–SAC2/MC–311G(2*d*,*d*,*p*)	1.2761	1.0797	1.090 5
Experiment	1.2746[a]	1.079[b]	1.091 ± 0.002[b]

[a] Reference 18.

[b] Reference 19.

TABLE II. Optimized transition state structures (C_{3v}) (bond lengths in Å and bond angles in degrees):

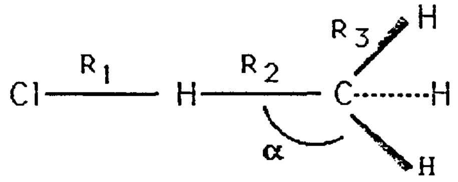

	R_1	R_2	R_3	α
HF/3–21G**	1.4896	1.3505	1.0757	102.37
HF/6–31G**	1.4903	1.3617	1.0774	102.49
HF/6–31 + G**	1.4944	1.3578	1.0775	102.46
HF/MC–311G(*d*,*d*,*p*)	1.5001	1.3537	1.0776	102.59
HF/MC–311G(2*d*,*d*,*p*)	1.5018	1.3501	1.0779	102.60
MP2/6–31G**	1.4265	1.3981	1.0796	101.66
MP2/6–31 + G**	1.4326	1.3915	1.0802	101.64
MP2/MC–311G(*d*,*d*,*p*)	1.4342	1.3870	1.0846	101.62
MP2/MC–311G(2*d*,*d*,*p*)	1.4473	1.3704	1.0847	101.57
MP–SAC2/MC–311G(2*d*,*d*,*p*)	1.4314	1.3881	1.0858	101.18

A well-known deficiency of unrestricted HF wave functions for doublets like CH_3 and the Cl–H–CH_3 transition state is that they are spin contaminated by higher multiplet states. However, in the present calculations the expectation value of S^2 in all UHF and MP2 wave functions for CH_3 and the transition state deviate from the correct value of 0.75 by at most 0.03. Since the spin contamination is found to be small, the UHF method is considered adequate to serve as a reference for perturbation theory and SAC calculations.

The optimized transition state structures for the Cl + CH_4 reaction predicted at the HF, MP2, and MP–SAC2 levels of calculation are shown in Table II. In the present study, we have assumed that the three atoms involved in bond breaking and bond making are colinear, i.e., the transition state has C_{3v} symmetry. As will be shown below, this is confirmed since the Hessian matrix of the C_{3v} transition state contains only one imaginary eigenvalue whose mode corresponds to the reaction coordinate of the Cl + $CH_4 \rightarrow CH_3$ + HCl reaction; thus it is in fact a true saddle point for the abstraction reaction. Notice that both the Cl–H (R_1) and H–C (R_2) bond lengths are increased in the HF/6–31G** structure as compared to the HF/3–21G** one. An additional set of *sp* diffuse functions on each heavy atom further increases the Cl–H and H–C (R_1 and R_2) bond distances in the HF/6–31 + G** structure. We also found that adding one more set of *d* polarization orbitals to the Cl atom in the MC–311G(2*d*,*d*,*p*) basis set does not change significantly the geometry of the HF transition state. However, the electron correlation included in the MP2 calculations generally decreases the Cl–H (R_1) and increases the H–C (R_2) bond distances, and this shifts the transition state closer to the product side (and concomitantly, as shown below, it lowers the barrier to activation). As expected, this trend is continued by the extrapolation procedure. The orientations of the three spectator hydrogen atoms is nearly the same in all HF and MP2 optimized structures.

Since the reaction is electronically about 7 kcal/mol endothermic, we would expect by Hammond's postulate[20] that the transition state would be somewhat product-like. Comparison of the bottom theoretical lines of Tables I and II shows that at the transition state the reactive C–H bond is elongated by 0.29 Å whereas the product H–Cl bond is elongated by only 0.16 Å, confirming this postulate as far as bond lengths are concerned. For bond angles, the transition state value of α is, however, only 41% of the way from the reactant value of 109.47° to the product value of 90°, and the spectator C–H bonds are only 44% of the way from reactants to products. Table III gives the vibrational frequencies and harmonic zero-point energies (ZPE) of the equilibrium structures of reactants and products at the highest level, MP2, at which we optimized structures, and for the largest, MC–311G(2*d*,*d*,*p*), basis set, and it compares these results to experiment.[19] The stretching frequency of HCl is 3048 cm^{-1} which is only 2% larger than the experimental value.[18] The frequencies of the CH_4 molecule are also overestimated, with the largest discrepancy being 199 cm^{-1} for the C–H symmetric stretch. These overestimates result in the harmonic zero point energy of the CH_4 molecule being 1.5 kcal/mol too large. The stretching, and doubly degenerate e' bending mode frequencies of CH_3 are also larger than experiment, by at most 187 cm^{-1}, but the low-frequency bending mode, which has no analog in CH_4, is 154 cm^{-1} *below* its correct value. Hence, the calculation overestimates the harmonic zero-point energy of CH_3 by less than 4%. In all cases, the Hessian matrix at the transition state has only one imaginary frequency mode which corresponds mainly (over 96%) to the motion of the hydrogen atom moving between two heavy nuclei Cl and C. The nature of the reaction coordinate plus the height of the barrier (see below) indicate that tunneling effects are probably important in the dynamics of this sytem at least under room-temperature thermal or other low-energy conditions.

We see that the HF vibrational frequencies all decrease by less than 100 cm^{-1} as the basis is improved from the 3–21G** to MC–311G(2*d*,*d*,*p*), and the imaginary frequency decreases from 1942*i* to 1846*i* cm^{-1}. However, including electron correlation in MP2 calculations very significantly changes the magnitude of these vibrational frequencies. There is reasonable agreement of the various MP2 and MP–SAC2 frequencies among themselves, i.e., comparing different bases, but, except for the ν_7 bend and the imaginary frequency mode, which is denoted $\nu_{\neq}$, the MP2 values are systematically lower than the HF ones. The largest difference in any of the values occurs for the imaginary–frequency mode which decreases from 1846*i* cm^{-1} (HF) to 949*i* cm^{-1} for the MC–311G(2*d*,*d*,*p*) basis set. The MP-SAC2/MC–311G(2*d*,*d*,*p*) imaginary frequency of 949*i* cm^{-1} can be compared with the value of 972*i* cm^{-1} which has been estimated from experiments with the bond-energy–bond-order (BEBO) model.[5] The two values are much closer than we have any right to expect. The imaginary frequency is of course very important in modeling the global potential surface for dynamical calculations. We conclude from Table IV that electron correlation is far more important than saturating the basis set in computing the vibrational frequencies of the transition state.

TABLE III. Vibrational frequencies (cm^{-1}) and zero-point energy (kcal/mol) at the MP2/MC–311G(2*d*,*d*,*p*) level.

	CH_3	CH_4	HCl
Calculated			
$\hbar\omega$	$3176(a_1')$	$3080(a_1)$	$3048(\sigma)$
	$426(a_2'')$	$1582(e)$	
	$3369(e')$	$3218(t_1)$	
	$1452(e')$	$1364(t_2)$	
ZPE	18.9	28.6	4.4
Experimental[a]			
$\hbar\omega$	$3002(a_1')$	$2917(a_1)$	$2991(\sigma)$
	$580(a_1'')$	$1534(e)$	
	$3184(e')$	$3019(t_1)$	
	$1383(e')$	$1306(t_2)$	
ZPE	18.2	27.1	4.3

[a] Reference 19.

It is tempting to make a new postulate, extending Hammond's to frequencies, i.e., for an endothermic reaction, the frequencies should be more product-like than reactant–like. Comparison of the final results (last column) of Table IV to the reactant and product frequencies of Table III shows some interesting features and provides a test of this postulate. First, both the symmetric and asymmetric C–H stretch frequencies of the saddle point are intermediate between the values for CH_4 and CH_3 and are 53–56% of the way between reactants and products, just barely in agreement with the new postulate. The next highest frequency is 96% of the way toward products. This makes the Fermi resonance much less resonant at the saddle point than for reactants. The umbrella mode of the transition state is only 93 cm^{-1} higher than the out–of–plane bend in CH_3.

B. Energetics

In the present study, we have employed the SAC method[11] in which an extrapolated result of order *n* is calculated by

$$E_{\mathrm{MP\text{-}SAC}n} = E_{\mathrm{HF}} + \frac{E_{\mathrm{MP}n} - E_{\mathrm{HF}}}{\mathscr{F}_n}, \tag{1}$$

where $\mathscr{F}_n$ is the scaling factor which is assumed constant, i.e., independent of geometry and/or bond rearrangement for a given system. To save space, we refer the reader to Ref. 11 for the motivation and physical basis of Eq. (1). Following the approach taken in previous work,[11] we have used accurate bond dissociation energies to estimate scaling factors, $\mathscr{F}_n$, by the following relation for each bond type:

$$\mathscr{F}_n = \frac{D_e(\mathrm{MP}n) - D_e(\mathrm{SCF})}{D_e(\mathrm{expt}) - D_e(\mathrm{SCF})}, \tag{2}$$

where the bond energy D_e refers to the energy difference for the reaction

$$\mathrm{AH}_n \rightarrow \mathrm{AH}_{n-1} + \mathrm{H}, \tag{3}$$

(A = Cl, C in this study). The energy for step (3) is ob-

TABLE IV. Transition state vibrational frequencies (cm^{-1}) and zero-point energies (kcal/mol).

Mode	3–21G**	6-31G**		6–31 + G**		MC–311G(*d,d,p*)		MC–311G(2*d,d,p*)		
	HF	HF	MP2	HF	MP2	HF	MP2	HF	MP2	MP-SAC2
$\nu_1(a')$	3283	3237	3194	3234	3184	3211	3132	3209	3131	3118
$\nu_2(a')$	1317	1292	1244	1293	1244	1287	1223	1288	1223	1227
$\nu_3(a')$	450	452	550	451	537	448	534	444	519	572
$\nu_4(e)$	3439	3391	3371	3388	3362	3361	3304	3359	3303	3295
$\nu_5(e)$	1552	1550	1491	1545	1478	1538	1456	1539	1457	1441
$\nu_6(e)$	1169	1120	973	1122	958	1086	920	1084	923	874
$\nu_7(e)$	428	421	389	425	388	383	328	381	337	324
$\nu_{\neq}(a')$	1942*i*	1870*i*	1270*i*	1868*i*	1298*i*	1845*i*	1242*i*	1846*i*	1163*i*	949*i*
ZPE[a]	26.1	25.7	24.9	25.6	24.8	25.3	24.2	25.3	24.2	24.0

[a] Harmonic.

tained from experiment (expt), SCF results, or the appropriate level of perturbation theory (MP*n*) for substitution into formula (2). The bond dissociation energies for H–Cl and H–C bonds for reaction (3) are given in Table V along with the resulting scaling factors $\mathscr{F}_n$ which are obtained by Eq. (2). The SCF bond dissociation energies are all much too low compared to experimental values, as expected. The scaling factors $\mathscr{F}_2$, and in two cases $\mathscr{F}_4$, are calculated at the MP2 optimized goemetries for various basis sets, and they indicate the fraction of the error recovered by including electron correlation. The $\mathscr{F}_n$ values for the C–H bond are generally larger than those for H–Cl bond. For some basis sets, the difference is rather significant, which means that this basis set is representing the electron correlation for C–H bond making better than that for H–Cl bond making. Striking examples of this lack of balance are provided by the 6–31G** basis set, for which $\mathscr{F}_2$ is 0.73 for H–Cl and 0.86 for C–H, and for which $\mathscr{F}_4$ is 0.74 and 0.91 for H–Cl and C–H bonds, respectively. Notice that the MC–311G(2*d,d,p*) basis set has the best "correlation balance" with $\mathscr{F}_2$ values of 0.83 and 0.84 for H–Cl and C–H bonds, respectively. The concept of correlation balance in basis sets has been introduced and discussed in a previous study by two of the authors.[23] Recall that the two exponential parameters for the *d* functions of the Cl atom in the MC–311G(2*d,d,p*) basis set are optimized with respect to the MP2 energy of the HCl molecule, hence increasing the $\mathscr{F}_2$ value for HCl bond. The good correlation balance of the basis set is a consequence of this optimization. For example, if we obtain the exponential parameters for these *d* functions by scaling the parameter of the MC–311G(*d,d,p*) basis set by factors of 1/2 and 2, which yields 0.375 and 1.5, the resulting $\mathscr{F}_2$ for the H–Cl bond is 0.80 as compared to 0.84 for C–H bond.

TABLE V. Theoretical bond dissociation energies (kcal/mol) and $\mathscr{F}_n$ parameter for MP–SAC calculations.

	H–Cl	$\mathscr{F}_n$	H_3C–H	$\mathscr{F}_n$
HF/3–21G**	76.9		88.3	
HF/6–31G**	75.3		84.6	
HF/6–31 + G**	75.4		86.1	
HF/MC–311G(*d,d,p*)	75.6		85.5	
MP2/6–31G**	97.4	0.73	109.2	0.86
MP2/6–31 + G**	97.7	0.73	107.8	0.81
MP2/MC–311G(*d,d,p*)	99.1	0.77	108.3	0.84
MP2/MC–311G(2*d,d,p*)	101.3	0.83	108.3	0.84
MP4/6–31G**//MP2[a]	98.1	0.74	110.5	0.91
MP4/MC–311G(*d,d,p*)//MP2[a]	99.9	0.80	109.7	0.89
Expt.	106.3[b]		112.7[c]	

[a] Single point MP4(SDTQ) calculations at MP2 optimized structures.

[b] Result is taken from Herzberg and Huber (Ref. 18).

[c] Results are taken from Gordon and Truhlar (Ref. 11).

The average values of the H–Cl and C–H scaling factors $\mathscr{F}_n$ are used in calculating the MP–SAC*n* barrier heights for the abstraction reaction Cl + $CH_4 \rightarrow CH_3$ + HCl and in the MP–SAC2/MC–311G(2*d,d,p*) optimizations. The total energies of the equilibrium and transition state structures are given in a table which is submitted as supplementary material, and the calculated classical barrier heights for both forward and reverse directions of the abstraction reaction are given in Table VI. The best available experimental estimated classical forward barrier height is probably that based on the BEBO model, which is about 8 kcal/mol.[5] (One of the goals of the present work is to characterize the saddle point well enough that an accurate semiglobal surface can be obtained and used to further refine this value.) The HF wave functions significantly overestimate the barrier heights in both the forward and reverse directions, as expected, even for large basis sets. Including electron correlation at the MP2 level decreases the forward barrier for all basis sets, by 42–69%, and the backward barrier by about 65–74%. This brings the predicted barriers into the correct ball park. Notice that the MP2 reverse barriers are less sensitive to the size of the basis set or the number of polarization functions included than are the forward barriers.

For the basis set with the best correlation balance, MC–311G(2*d,d,p*), which is also the largest basis set among those being considered, the MP2 forward and reverse barriers are 10.2 and 3.2 kcal/mol, respectively. Including harmonic zero-point energy corrections reduces the forward barrier to 5.8 kcal/mol, while it raises the reverse barrier to 4.1 kcal/mol. Thus the heat of reaction at 0 K predicted at the MP2 level using MC–311G(2*d,d,p*) basis set is 1.7 kcal/mol. This is, in fact, in excellent agreement with the experimental heat of reaction $\Delta H^\circ = 1.89 \pm 0.10$ kcal/mol.[6] Since

TABLE VI. Calculated barrier heights (kcal/mol) for the Cl + $CH_4 \rightarrow HCl + CH_3$ reaction.

Basis	HF	MP2	MP4//MP2[a]	MP-SAC2//MP2[a]	MP-SAC2	MP-SAC4//MP2[a]
Forward barrier						
3-21G**	22.2					
6-31G**	22.6	8.8	15.4	4.8		13.9
6-31 + G**	22.4	7.8		3.4		
MC-311G(*d,d,p*)	21.9	12.8	13.2	10.6		11.6
MC-311G(2*d,d,p*)	21.7	10.2		7.9	7.9[b]	
Reverse barrier						
3-21G**	10.9					
6-31G**	10.7	3.1	3.1	1.1		1.5
6-31 + G**	11.9	4.2		1.9		
MC-311G(*d,d,p*)	11.9	3.6	3.4	2.0		1.8
MC-311G(2*d,d,p*)	12.2	3.2		1.4	1.2[b]	

[a] Single point MP4 and MP-SAC*n* calculations at MP2 optimized structures.

[b] Best value.

this basis is well correlation balanced the SAC2 extrapolation changes the heat of reaction very little, in particular by less than 1 kcal/mol.

The MP4 single point energies appear less accurate than the MP2 optimized ones. They overestimate the forward barrier by 5–8 kcal/mol relative to the estimated experimental values of 8 kcal/mol, although they make similar predictions to MP2 for the reverse barrier.

Finally, the MP-SAC*n* barrier heights are also listed in Table VI. The most reliable estimates would be expected to be those calculated from the most correlation balanced basis set at the highest level of perturbation theory available for that basis set, that is, in the present study, the MP-SAC2/MC-311G(2*d,d,p*) level. At this level, the MP-SAC2 forward and reverse barriers are 7.9 and 1.2 kcal/mol, respectively. Adding the MP2 harmonic zero-point energy corrections to the forward barrier yields the vibrationally adiabatic ground-state barrier height, which has a value of 3.5 kcal/mol; and the zero-point-corrected reverse barrier height is 2.3 kcal/mol. The forward barrier is in excellent agreement with the experimental activation energy of 3.5 kcal/mol in the range of 360–500 K.[5] Actually, because of tunneling, the experimental activation energy might be less than the true zero-point-corrected barrier, so our calculated barrier might be slightly too low. In addition, at 0 K, the MP-SAC2 heat of reaction, 1.2 kcal/mol, is within 0.7 kcal/mol of the experimental value mentioned above.

It is very interesting to notice from Table V that the 6-31G** and MC-311G(*d,d,p*) basis sets are better correlation balanced ($\mathscr{F}_n$ values for C–H and H–Cl are closer together) at the MP2 than at the MP4 level. As a result, as seen in Table VI, the barrier heights calculated at the MP2 level using these basis sets are closer to the best values than those calculated at the MP4 level. This is also true for the MP-SAC2 results as compared to the MP-SAC4 results. Thus, the degree of basis set correlation balance, or lack thereof, for all active bonds in the system provides another explanation for why higher-order perturbation theory sometimes predicts less accurate barrier heights than lower-order calculations. This has a significant implication for the optimum strategy for selecting a combination of basis set and correlation level for an *ab initio* calculation; that is, when including correlation energy in calculating the barrier height for a reaction, one should use the best possible correlation balanced basis set for each level of theory.

IV. SUMMARY AND CONCLUSIONS

We have calculated forward and reverse barrier heights of 7.9 and 1.2 kcal/mol, respectively, for the title reaction,

TABLE VII. Supplementary material for "Transition state structure, barrier height, and vibration frequencies for the reaction Cl + $CH_4 \rightarrow CH_3$ + HCl" by T. N. Truong, D. G. Truhlar, K. K. Baldridge, and M. S. Gordon, and R. Steckler.

	Cl	HCl	CH_3	CH_4	$Cl\cdots H\cdots CH_3$(TS)
HF/3-21G**	− 457.371 093	− 457.989 877	− 39.360 708	− 39.997 564	− 497.332 16
HF/6-31G**	− 459.447 964	− 460.066 214	− 39.564 457	− 40.201 705	− 499.613 530
HF/6-31 + G**	− 459.455 871	− 460.067 364	− 39.566 699	− 40.202 131	− 499.615 160
HF/MC-311G(*d,d,p*)	− 459.477 155	− 460.097 386	− 39.572 928	− 40.209 024	− 499.651 294
HF/MC-311G(2*d,d,p*)	− 459.478 582	− 460.099 652	− 39.572 928	− 40.209 024	− 499.653 054
MP2/6-31G**	− 459.562 057	− 460.215 621	− 39.697 533	− 40.369 856	− 499.908 218
MP2/6-31 + G*	− 459.564 333	− 460.218 261	− 39.701 211	− 40.371 223	− 499.912 909
MP2/MC-311G(*d,d,p*)	− 459.638 402	− 460.296 155	− 39.727 600	− 40.399 967	− 500.018 003
MP2/MC-311G(2*d,d,p*)	− 459.665 294	− 460.326 120	− 39.727 600	− 40.399 967	− 500.048 957
MP4/6-31G**//MP2[a]	− 459.578 818	− 460.233 376	− 39.719 561	− 40.393 850	− 499.948 061
MP4/MC-311G(*d,d,p*)//MP2[a]	− 459.656 299	− 460.312 90	− 39.752 037	− 40.426 682	− 500.061 892
MP-SAC2/MC-311G(2*d,d,p*)	− 459.702 144	− 460.370 857	− 39.758 177	− 40.437 716	− 500.127 161

[a] MP4(SDTQ) single-point calculations at the optimized MP structures with the same basis set.

using the MP–SAC2 level of theory. The forward barrier height appears to be in excellent agreement with experiment. In arriving at the final value, we compared several calculations with various levels of electron correlation and basis set size, and we made some observations that may have general implications for theoretical studies of reaction dyamics. First, we found that the electron correlation is very important not only for predicting the classical barrier heights but also in calculating the vibrational frequencies, especially the imaginary frequency of the transition state. Second, we found that if the basis set being used is correlation balanced for both bonds involved in the reaction, scaling the correlation energy greatly improves the barrier predictions, and in particular scaling the correlation energy in a well-balanced MP2 calculation yields better results than a (much more expensive) MP4 single-point calculation. Third, we showed that several of the widely used basis sets are not correlation balanced; we found it necessary to use two *d* sets on Cl to achieve a fully polarized, correlation–balanced basis set for the title reaction.

Finally, we found that Hammond's postulate holds for bond lengths of bond breaking and bond making coordinates but not for bond angles and spectator C–H bond lengths. Since different coordinates proceed from reactants to products at different rates, even for this simple concerted reaction, one must always be careful about using interpolated structure parameters at transition states.

Table VII gives absolute energies in hartrees.

ACKNOWLEDGMENTS

The authors are grateful to Michael W. Schmidt for assistance with the calculations. This work was supported in part by the National Science Foundation, the Minnesota Supercomputer Institute, the Air Force Office of Scientific Research, and the San Diego Supercomputer Center.

[1] F. S. Rowland and M. J. Molina, Rev. Geophys. Space Phys. **13**, 1 (1975).
[2] D. A. Whytock, J. H. Lee, J. V. Michael, W. A. Payne, and L. J. Stief, J. Chem. Phys. **66**, 2690 (1977).
[3] C. L. Lin, M. T. Len, and W. B. DeMore, J. Phys. Chem. **82**, 1772 (1978).
[4] L. F. Keyser, J. Chem. Phys. **69**, 214 (1978).
[5] M. S. Zahniser, B. M. Berquist, and F. Kaufman, Int. J. Chem. Kinet. **10**, 15 (1978).
[6] O. Dobis and S. W. Benson, Int. J. Chem. Kinet. **19**, 691 (1987).
[7] S. P. Heneghan, P. A. Knoot, and S. W. Benson, Int. J. Chem. Kinet. **13**, 677 (1981).
[8] D. G. Truhlar, R. Steckler, and M. S. Gordon, Chem. Rev. **87**, 217 (1987).
[9] J. S. Binkley and J. A. Pople, Int. J. Quantum Chem. **9**, 229 (1975); J. A. Pople, J. S. Binkley, and R. Seeger, *ibid.* **10**, 1 (1976).
[10] R. Krishnan and J. A. Pople, Int. J. Quantum Chem. **14**, 91 (1980).
[11] M. S. Gordon and D. G. Truhlar, J. Am. Chem. Soc. **108**, 5412 (1986).
[12] M. S. Gordon, J. S. Binkley, J. A. Pople, W. J. Pietro, and W. J. Hehre, J. Am. Chem. Soc. **104**, 2797 (1982); J. S. Binkley, J. A. Pople, and W. J. Hehre, *ibid.* **102**, 939 (1986); W. J. Pietro, M. M. Francl, W. J. Hehre, D. J. DeFrees, J. A. Pople, and J. S. Blinkley, *ibid.* **104**, 5039 (1982).
[13] M. J. Frisch, J. A. Pople, and J. S. Binkley, J. Chem. Phys. **80**, 3265 (1984).
[14] R. Krishnan, J. S. Binkley, R. Seeger, and J. A. Pople, J. Chem. Phys. **72**, 650 (1980).
[15] A. D. McLean and G. S. Chandler, J. Chem. Phys. **72**, 5639 (1980).
[16] J. S. Binkley, M. J. Frisch, D. J. DeFrees, R. Krishnan, R. A. Whiteside, H. B. Schlegel, E. M. Fluder, and J. A. Pople, GAUSSIAN82, Carnegie-Mellon University, Pittsburgh, PA, 1983.
[17] M. J. Frisch, J. S. Binkley, H. B. Schlegel, K. Raghavachari, C. F. Melius, R. L. Martin, J. J. P. Stewart, F. W. Bobrowicz, C. M. Rohlfing, L. R. Kahn, D. J. DeFrees, R. Seeger, R. A. Whiteside, D. J. Fox, E. M. Fluder, and J. A. Pople, GAUSSIAN82, Carnegie-Mellon Quantum Chemistry Publishing Unit, Pittsburgh, PA, 1984.
[18] G. Herzberg and K. P. Huber, *Molecular Spectra and Molecular Structure. IV. Constants of Diatomic Molecules* (Van Nostrand, Princeton, NJ, 1979).
[19] *JANAF Thermochemical Tables*, 3rd Ed., edited by M. W. Chase, Jr., C. A. Davies, J. R. Downey, Jr., D. J. Frurip, and R. A. McDonald (Natl. Stand. Ref. Data Ser. Natl. Bur. Stand., 1985), Vol. 14.
[20] G. S. Hammond, J. Am. Chem. Soc. **77**, 334 (1955).
[21] R. T. Skodje and D. G. Truhlar, J. Phys. Chem. **85**, 624 (1981).
[22] R. T. Skodje, D. G. Truhlar, and B. C. Garrett, J. Phys. Chem. **85**, 3019 (1981).
[23] M. S. Gordon and D. G. Truhlar, Int. J. Quantum Chem. **16**, 81 (1987).